Int. J. Solids Structures, 1977, Vol.13, pp. 865–876. Pergamon Press. Printed in Great Britain

NUMERICAL ANALYSIS OF LARGE ELASTIC-PLASTIC DEFORMATION OF BEAMS DUE TO DYNAMIC LOADING†

A. SPERLING and Y. PARTOM

Material Mechanics Laboratory, Faculty of Mechanical Engineering, Technion, Israel Institute of Technology, Haifa, Israel

(*Received* 29 *March* 1976; *revised* 6 *December* 1976)

Abstract—Numerical calculations were performed for two examples of the response of elastic-plastic beams subjected to dynamic loads. These were a simply supported, axially restrained beam under suddenly applied uniform pressure, and an axially restrained, clamped beam with a central mass that is impacted by a projectile. Large elastic-plastic deflections were considered, and the method of finite differences was used. Two different constitutive equations were assumed: the elastic-perfectly plastic relation, and a special elastic-viscoplastic, strain hardening model. Analysis of the results included examining the interaction between the bending moment and the axial force, the variation of the axial force, bending moment and deflection with time, and the propagation velocities of the various phenomena during motion. Experiments were carried out in which a rifle projectile hit a central mass which had been fastened to a clamped beam. Comparison between the theoretical and experimental dynamic deflections shows good agreement for relatively short response times.

INTRODUCTION

The beam is one of the simplest structures and, therefore, many studies have been carried out to determine its response to transversely applied dynamic loads. In the case of large elastic-plastic deformation, the problem cannot be solved exactly by analytical methods as it becomes relatively complicated.

There are a number of analytical and experimental investigations which deal with simple beam problems in which the analyses generally assume rigid-plastic or elastic-perfectly plastic behavior of the material, e.g. Parkes[1], Nonaka[2]. For more information, Symonds[3] gives a very detailed survey of analytical methods and experimental results. For complicated boundary conditions or more realistic constitutive equations, numerical methods must be used to obtain results for the dynamic behavior of beams.

In the present investigation, the method of finite differences was used based on the work of Leech and Pian[4] and Witmer, Balmer, Leech and Pian[5]. It is suitable for any set of boundary conditions, and any constitutive equation may be used. The main aim of the present work was to study several aspects of the response characteristics of beams of elastic, viscoplastic material such as the deflection curve as a function of time, the final deflection, the interaction between the axial force and the bending moment, the propagation velocities of the various phenomena, etc.

One of the important points in such problems is to characterize the dynamic, inelastic material behavior by defining its constitutive equation. This subject has been extensively studied during the last two decades because many practical problems require this information. Review papers on this subject have been written by Lindholm[6], Campbell[7] and by others.

It has seemed expedient to develop a material representation which is not based on a yield condition and which is rate dependent in the complete range of stress states. Such a formulation would have more physical basis than the classical idealizations and would be more suitable for numerical computations. Bodner and Partom[8, 9] have recently developed constitutive equations for elastic viscoplastic, strain hardening materials which do not require a yield criterion and are motivated by dislocation dynamics. It is specially suitable for numerical procedures since neither unloading nor yielding conditions have to be introduced. An important part of this work is the application of the Bodner and Partom theory to the beam problem and to compare the results to experimental work and to theoretical predictions obtained by assuming elastic-perfectly plastic material behavior.

†The research reported in this document has been supported in part by the Air Force Office of Scientific Research under Grant AFOSR-74-2607B, through the European Office of Aerospace Research (EOAR), United States Air Force.

STRUCTURAL ANALYSIS

A general model for large dynamic deflections of shells was developed by Leech and Pian[4], and by Witmer, Balmer, Leech and Pian[5], which is directed to numerical solutions by the method of finite differences. The basic equations are Newton's second law for a segment of a beam which is considered as the basic structural element. The analysis takes into account large deflections and strains, both tangential or lateral loadings, and can be used with any constitutive equation of the material. On the other hand, the beam element was assumed to be "long" so that shear deformation and rotational inertia could be neglected. Motion in one plane was considered as well, and changes in cross sectional area were neglected.

The dynamic model consists of point masses which are connected by straight weightless rods. The rods' length may change according to the axial force, but the rods never bend. Any change in curvature can take place only by changing angles between the rods. The beam cross section is represented by horizontal layers which are connected by a vertical web. This web has no axial strength but it is perfectly rigid against shearing stresses. The properties of the modified cross section must be equivalent to those of the original one. Therefore, the total cross sectional area of the layers must be equal to that of the original beam. The second requirement is that the modified cross section has the same resistance against bending, both in the elastic and inelastic ranges, as the original cross section. This can be achieved only by taking a sufficiently large number of layers. A detailed description of the dynamic model and the dynamic and geometric relations is given in [4, 5].

To achieve good computational results, it was found that some of the kinematic relations have to be written in a form different from the obvious one. This is due to the limited accuracy of the digital computer. It was observed that some variables computed by kinematic relations were given the value zero instead of their relatively small value. This was a consequence of the normal advance and development of the following steps of calculation and could occur when calculating a relatively small value as a difference between two large values. The best example is the increase of strain of the neutral axis $\Delta\epsilon_i^r$ after one time increment, where i denotes the segment number along the beam and r is the number of the time increment. Usually, the strain increase is given by

$$\Delta\epsilon_i^r = \frac{\Delta(\delta S)_i^r}{\delta X} = \frac{\delta S_i^r - \delta S_i^{r-1}}{\delta X} \tag{1}$$

where X is the coordinate along the original axial direction of the beam, δX is the initial length of one segment of the beam, δS_i^r is the length of the ith segment after r time increments, and Δ denotes an increment of any variable due to one time increment ΔT. δS_i is given by the coordinates of the point masses

$$(\delta S_i)^2 = (X_i - X_{i-1})^2 + (Y_i - Y_{i-1})^2. \tag{2}$$

It was realized that eqns (1) and (2) are not suitable for the numerical procedure, mainly in the early steps, because the difference calculated in eqn (1) is very small in comparison with the segment length. This causes the computer to neglect the strain from the beginning with the result that no stress is "developed" during the entire calculation and the program fails. This difficulty is avoided if the strain increase is calculated directly from the point mass velocities. By time differentiation of (2) we get for the strain increase:

$$\Delta\epsilon_i = [\cos\theta_i(\dot{X}_i - \dot{X}_{i-1}) + \sin\theta_i(\dot{Y}_i - \dot{Y}_{i-1})]\Delta T/\delta X \tag{3}$$

where $\dot{X}_i$, $\dot{Y}_i$ are the velocities, and θ_i is the angle between the ith rod of the dynamic model and the x-axis. The same procedure was carried out to compute the curvature increase directly from the velocities.

The calculation of the geometric variables by their change with time, instead of by those relations which had been used before, leads to fairly accurate values for the strain increase of every layer. From the segment geometry

$$\delta\bar{S} = \delta S(1 + \xi K) \tag{4}$$

where ξ is the distance of the layer from the neutral axis, K is its curvature, and the bar over any given parameter denotes that the value corresponds to a single layer. The time differentiation of eqn (4) gives the formula for the increase of strain of the kth layer, which is important for large deflections and curvatures:

$$\Delta\bar{\epsilon}_i(k) = \Delta[\delta\bar{S}_i(k)]/\delta X = \Delta\epsilon_i[1 + \xi(k)K_i] + \frac{\delta S_i}{\delta X}\xi(k)\Delta K_i. \tag{5}$$

The relation for the deformation rate $\bar{d}$ is:

$$\bar{d}_i(k) = \Delta[\delta\bar{S}_i(k)]/\delta\bar{S}_i(k)\Delta T \tag{6}$$

BOUNDARY CONDITIONS

Numerical computations were carried out for two examples: (A) A simply supported, axially constrained beam subjected to suddenly applied uniform pressure which remains constant with time. (B) A fully clamped, axially constrained beam with a central mass subjected to projectile impact and imbedment in the mass.

Example A was chosen as it is a typical and classical problem so that general conclusions can be derived from it about the dynamic behavior of the variables. Another reason is that this example is relatively simple to solve analytically for low loads for which the beam is in the elastic range. It was of interest to compare the general program results for the elastic range to the corresponding analytical solution for elastic vibrations.

Example B was chosen as it is a relatively simple experimental arrangement. Experiments were carried out and the results of the theoretical and experimental mid-beam deflections were compared. Figure 1 gives the drawing of the specimen. As the central mass was assumed to be concentrated at midpoint, it is obvious that

$$m_m = m_0 + m_i + m_b \tag{7}$$

where m_m is the total midpoint mass, m_0 is the projectile mass, m_i is the point mass of the homogeneous beam, and m_b is the mass of the blocks, bolts and nuts.

For the first approximation, the impulse was assumed to occur in a very short time so that the mid-beam initial velocity is given by

$$v_m^0 = m_0 V_0/m_m \tag{8}$$

where V_0 is the projectile impact velocity. Secondly, it was assumed that the impulse acts during a finite time T_1 so that the average force is

$$F_1 = m_0 V_0/T_1. \tag{9}$$

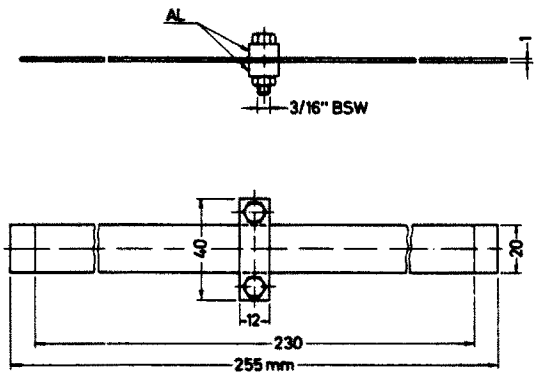

Fig. 1. Drawing of the experimental specimen.

As T_1 has a relatively small value (in microseconds), almost the same results were obtained for both assumptions when longer deformation times were considered.

CONSTITUTIVE EQUATIONS

The two examples were solved assuming two different relations for the constitutive equations:

(1) Elastic-perfectly plastic (e.p.p.).

(2) Elastic-viscoplastic, strain hardening (e.v.p.) which has been developed within the last years by Bodner and Partom [8, 9].

The e.p.p. relation is the simplest and most economical one from the computational viewpoint, but is considered only as a first approximation to actual material behavior. For better predictions, some other relations might be used such as the elastic linear strain hardening (bilinear) relation [5] or a Ramberg–Osgood type representation which takes into account the strain hardening phenomenon. If the material shows significant strain rate sensitivity, some approximation for this effect can be made, and there are suggestions for such strain rate laws, e.g. Bodner and Symonds [10]. The beam problems under consideration involve loading and unloading and the strain rate changes with time and place along the beam. Even in the same cross section, the strain rate varies for every layer so the preceding methods cause computational difficulties and an expenditure of computation time.

A theory of elastic-viscoplastic, strain hardening material behavior which does not require a yield criterion or loading and unloading conditions would be very useful for this class of dynamic plasticity problems. These characteristics are inherent in the theory developed by Bodner and Partom [8, 9] which is motivated in part from concepts of "dislocation dynamics". One of the important points in the present paper has been to examine some consequences of using this theory for structural problems involving loading and unloading and changing strain rates.

The basic assumption of the theory is that the total deformation rate can be separated at all stages into elastic and inelastic components,

$$d_{ij} = d_{ij}^e + d_{ij}^p \tag{10}$$

where

$$d_{ij} = \frac{1}{2}(V_{i,j} + V_{j,i}) \tag{11}$$

and V_i are the particle velocity components. This leads to constitutive equations in which the rate components are functions only of state variables, e.g. the elastic stress, and the deformation state.

The basic form of the flow law of classical plasticity is:

$$d_{ij}^p = \underline{d}_{ij}^p = \lambda \underline{\sigma}_{ij} \tag{12}$$

where the bar symbol indicates the deviatoric components.

Squaring (12) leads to

$$\lambda^2 = D_2^p / J_2 \tag{13}$$

where D_2^p and J_2 are the second invariants, respectively, of the plastic deformation rate deviator and the elastic stress deviator. It is further assumed that

$$D_2^p = f(J_2). \tag{14}$$

Suggested forms for this function are those that have been developed to relate the dislocation velocity to the stress. Equation (14) can then be interpreted as a multi-dimensional generalization of those unidirectional equations. A convenient form for eqn (14) that appears to

have a physical basis was proposed by Bodner and Partom [8, 9],

$$D_2^p = -D_0^2 \exp\{-[A^2/(-J_2)]^n\} \tag{15}$$

where

$$A^2 = (1/3)Z^2\left(\frac{n+1}{n}\right)^{1/n}. \tag{16}$$

The quantities D_0, Z and n are material constants. Work hardening is considered by making Z an increasing function of the quantity that represents the worked state of the material which, for simplicity, is taken to be the total plastic work W_p, where

$$\dot{W}_p = \sigma_{ij} d_{ij}^p. \tag{17}$$

This would correspond to the plastic deformation rate being a decreasing function of W_p which is one of the macroscopic consequences of strain hardening. A suitable functional form for $Z = Z(W_p)$ is

$$Z = Z_1 + (Z_0 - Z_1)\exp(-mW_p/Z_0) \tag{18}$$

where Z_0, Z_1, and m are new material constants. This hardening law corresponds to isotropic hardening and therefore does not indicate any Bauschinger effect.

The beam problems in the present paper were considered to have only uniaxial stress, for which

$$J_2 = -\frac{\sigma^2}{3} \tag{19}$$

where σ is the axial stress in a layer of the beam, and

$$\sigma_{11} = 2\sigma/3. \tag{20}$$

The expression for the axial plastic deformation rate is obtained from (12), (15), (19) and (20),

$$d^p = \lambda\sigma_{11} = \frac{2D_0}{\sqrt{3}}\frac{\sigma}{|\sigma|}\exp\left[-\frac{1}{2}(3A^2/\sigma^2)^n\right]. \tag{21}$$

The rate of plastic work is derived from (17),

$$\dot{W}_p \simeq \sigma d^p \tag{22}$$

and the elastic deformation rate is given by Hooke's Law for the case of small elastic strains,

$$d^e = \dot{\sigma}/E. \tag{23}$$

The stress σ can then be computed from these equations by an iteration method in which the total axial deformation rate d is calculated by the coordinates and velocities of the point masses and both d^e and d^p are given functions of $\dot{\sigma}$ and σ.

EXPERIMENTAL WORK

The case of a fully clamped beam with a central mass subjected to an impulsive force at the mid-point was investigated experimentally. The impulse was applied by a bullet striking and imbedding itself in the central mass, and high speed photographs were taken of the beam response.

The projectile was a standard 0.22 in caliber bullet having a mass of 2.63 gr and an average

velocity of 400 m/sec. It was made of lead and covered with brass. Figure 1 is a detailed drawing of the specimen where the central mass consists of two aluminum blocks bolted to the beam mid-point. The weight of these two blocks plus the two bolts and nuts was about 30 gr. The beam total length was 255 mm, but as it was clamped at its ends, the effective length was 230 mm. Its width was 20 mm and thickness 1 mm.

Experiments were carried out for two materials: Al 6061-T6 and commercially pure titanium. A large number of tests were performed on 16 specimens in order to get reliable results.

Figure 2 is a schematic of the experimental arrangement. The system included three flash units which were inter-connected by time delay units so that three flashes—one after the other—could be carried out with maximum available time intervals of 150 μsec. Every picture, therefore, can include three dynamic positions of the deflected beam so that the exact time for each position can be readily calculated. Pictures of the final static deflection were also taken.

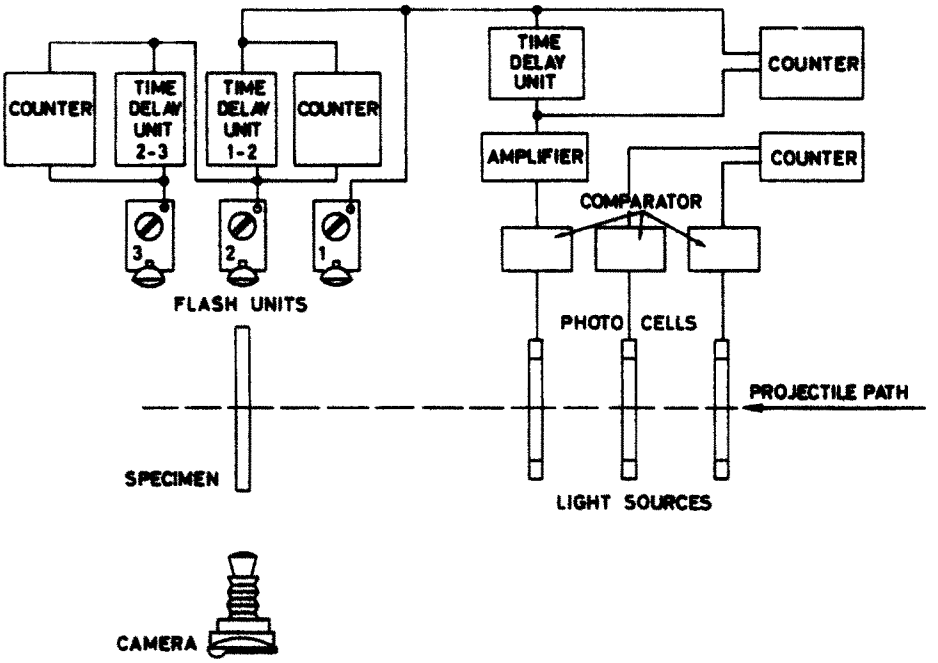

Fig. 2. Schematic of the experimental arrangement.

RESULTS AND CONCLUSIONS

Mechanical properties

The mechanical properties of the materials were obtained by tensile experiments in an Instron testing machine. It was realized that the strain rate sensitivity of Al 6061-T6 is very small and can be ignored and its strain hardening is also negligible. Therefore, it was considered in the computations as an elastic perfectly plastic material with an average yield stress of 30 kg/mm^2.

Figure 3 shows stress-strain curves for commercially pure titanium. It can be seen that it has high rate sensitivity and its strain hardening is not large but cannot be neglected. Therefore, it has to be treated in computations as an elastic-viscoplastic, strain hardening material. This material, as mentioned before, is defined by five material constants (in addition to its elastic modulae): D_0, Z_0, Z_1, n and m, which can be obtained by fitting results of uniaxial tensile experiments to those computed numerically. Figure 3 shows the graphs obtained by fitting results at two relatively low strain rates. The upper curve is an extrapolation for a higher rate of 10 sec^{-1}. The following values were obtained for titanium:

$$D_0^2 = 10^8 \text{ sec}^{-2}$$
$$n = 1$$
$$m = 100$$

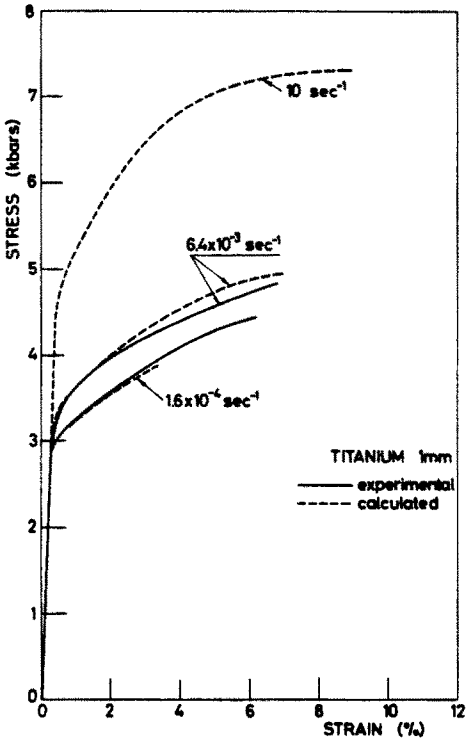

Fig. 3. Stress-strain relation of a titanium specimen during tensile test.

$$Z_0 = 12.6 \text{ Kbars}$$
$$Z_1 = 19.5 \text{ Kbars}$$

These properties are similar to those obtained in the past works except for Z_0 and Z_1 which here have higher values. Since the important strain rates for the beam response in the impulsive loading tests were in the high range, about 10 sec^{-1}, it would have been preferable to choose the material constants to best fit results in this range. However, these were not available for the specimen material. Other test data on titanium, e.g. [11], indicate that the calculated stress-strain curve for $\dot{\epsilon} = 10 \text{ sec}^{-1}$, Fig. 3, is reasonable at low strain levels but somewhat over-magnifies the strain hardening effect at high strains.

In order to compare the elastic-viscoplastic, strain hardening material behavior to that of the elastic-perfectly plastic material, it was necessary to assume an approximate average value for the yield stress σ_0 of titanium. The results of the numerical examples for the response of the beams shows that the principal strain rates were about 10 sec^{-1}. The calculated stress-strain relation for this rate, Fig. 3, indicates that the "yield stress" for large strains would be approximately 7.3 Kbar.

Theoretical results for example A

For the numerical example of a simply supported beam under suddenly applied uniform pressure which remains constant with time, a titanium beam with a length of 100 cm and a square cross section of 2×2 cm was considered. The beam was divided into 40 segments and 4 layers for the numerical procedure. A uniformly distributed force of 4×10^9 dyn/cm was assumed to be applied suddenly to the lateral surface of the beam. Only numerical studies were performed for this example as a suitable experimental system for uniform dynamic load application was not available.

Figure 4 shows the calculated axial force at mid-beam as a function of time. Since its appearance starts at the supports and then moves towards mid-beam, the force at the middle becomes non-zero only after a time of about 100 μsec. The average velocity of this signal is, therefore,

$$V_1 = 0.5 \text{m}/100 \times 10^{-6} \text{ sec} = 5000 \text{ m/sec.} \tag{24}$$

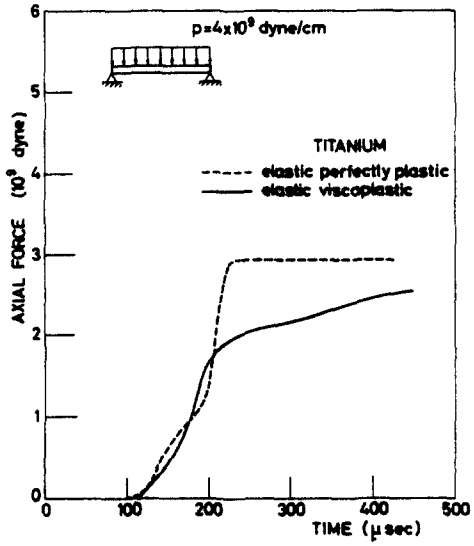

Fig. 4. Axial force at center of a simply supported axially constrained titanium beam, subjected to a uniform step load.

The velocity of the elastic wave is

$$V_e = \sqrt{(E/\rho)} = \sqrt{\left(\frac{1.2\times 10^{12}\,\mathrm{dyn/cm^2}}{4.87\,\mathrm{gr/cm^3}}\right)} = 4960\ \mathrm{m/sec}. \tag{25}$$

It is obvious that $V_1 \simeq V_e$ as had been expected.

Figure 5 shows the axial force at the end of the beam as a function of time. A principal difference between Figs. 4 and 5, aside from the time response factor, is the final value of the axial force for the e.v.p. material. At mid-beam it is less than that of the e.p.p. material, but at the beam end it is much higher. This is a consequence of an average value being assumed for the yield stress of the e.p.p. material, and the strain rates at the ends being higher than those at the middle. Because of this variation, the e.v.p. relation would give more realistic results for a rate sensitive material.

Figure 6 gives the bending moment 5 cm from the beam end as a function of time. The curve

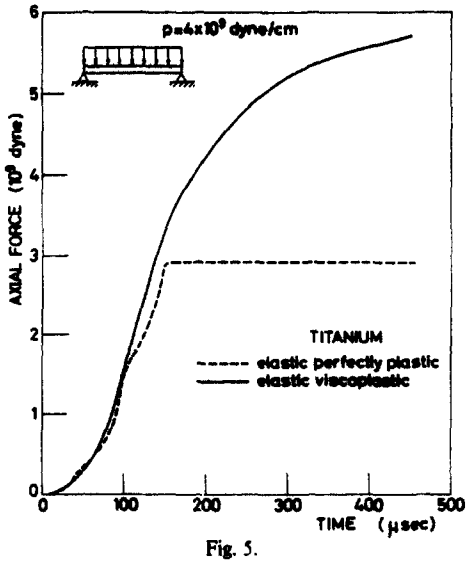

Fig. 5.

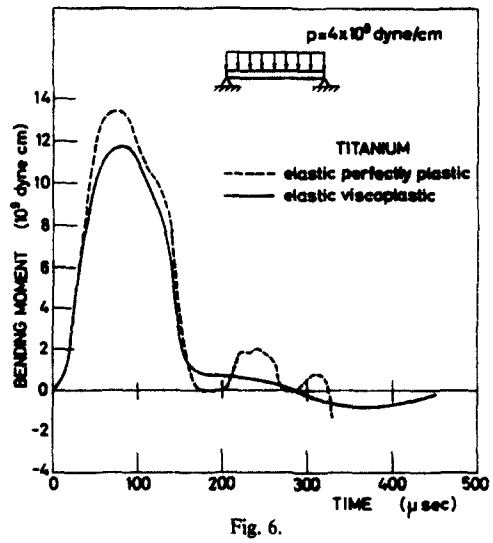

Fig. 6.

Fig. 5. Axial force at the end of a simply supported axially constrained titanium beam, subjected to a uniform step load.

Fig. 6. Bending moment 5 cm from the end of a simply supported axially constrained titanium beam, subjected to a uniform step load.

for the e.v.p. material is more "smooth" and seems to represent the real physical behavior more correctly.

The relation between the bending moment M and the axial force N for a rectangular cross section and an elastic perfectly plastic material is given for complete yielding of the whole cross section by

$$\left|\frac{M}{M_p}\right| + \left[\frac{N}{N_p}\right]^2 = 1 \tag{26}$$

when M_p is the fully plastic moment and N_p is the fully plastic axial force. As M_p and N_p are constants of the cross section, eqn (26) is a direct connection between M and N for the fully plastic range. If N reaches N_p, then M becomes zero and the beam behaves like a string. In the present problem, most of the cross sections along the beam are not in a situation of complete yielding, but it is still of interest to check this relation. It was done for the e.p.p. material, as shown in Figs. 7–9, which represent pictures of M, N and the deflection Y in different times. At the start of beam motion, the axial force is very small but then starts growing with time. When the deflection is about 7.5 cm, the beam behaves almost like a string as can be seen in Fig. 9.

An interesting phenomenon is the deflection curve in Figs. 8 and 9 which has its highest value near the beam ends and not at the middle. The same effect can be observed in photographs of the experiments of Florence and Firth[12].

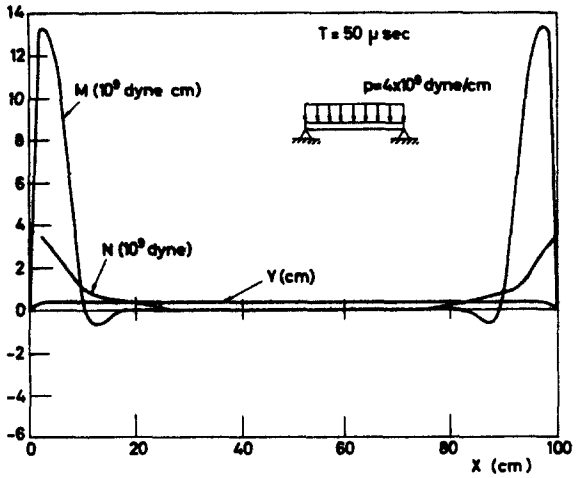

Fig. 7. Bending moment, axial force and deflection of a simply supported axially constrained elastic-perfectly plastic titanium beam, 50 μsec after application of a uniform step load.

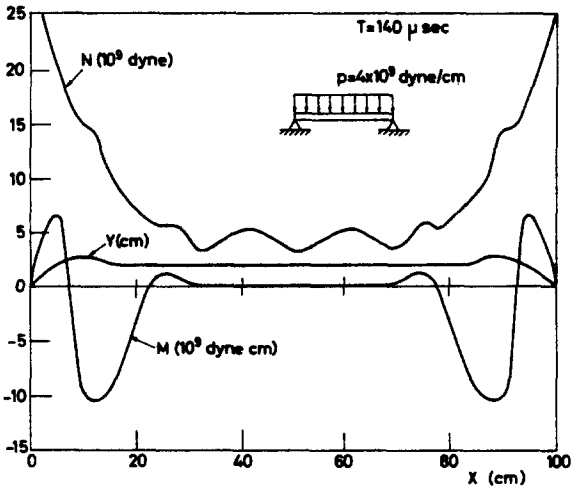

Fig. 8. Bending moment, axial force and deflection of a simply supported axially constrained elastic-perfectly plastic titanium beam, 140 μsec after application of a uniform step load.

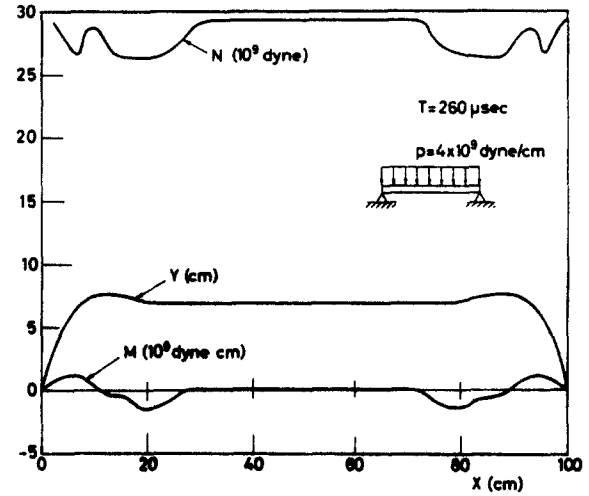

Fig. 9. Bending moment, axial force and deflection of a simply supported axially constrained elastic-perfectly plastic titanium beam, 260 μsec after application of a uniform step load.

Theoretical and experimental results for example B

Experiments and calculations for this case were carried out for both A1 6061-T6 and commercially pure titanium. Figure 10 shows the calculated response shapes of one half the titanium beam at different times. It was treated as an e.v.p. material. Smaller overall deflections were obtained for the titanium beam than for the AL 6061-T6 beam because of the rate sensitivity factor. In addition, the deflected shapes of the titanium beams were more curved than those for the aluminum beams for which almost straight lines were obtained. The negative deflection near the two ends of the deflected zone was also observed in the experimental photographs.

Figure 11 compares the experimental mid-beam deflection to the calculated deflection as a function of time for titanium. The experimental points are above the theoretical curve. This is probably a consequence of the material parameters being obtained by fitting results for low strain rates. Here the behavior is extrapolated to much higher strain rates which may cause accuracy problems. Final deflection magnitudes were not computed due to the long computer times involved.

Figure 12 shows how the length of the deflected zone increases with time in aluminum. There is good agreement between the calculations and the experiment except for the final state. This disagreement is caused by the fact that the dynamic model consisted of straight segments with finite length so the boundary conditions for clamped ends of the beam makes the effective length of the deflecting beam shorter with the result that the theoretical $\bar{Z}$ cannot reach the value of the total length.

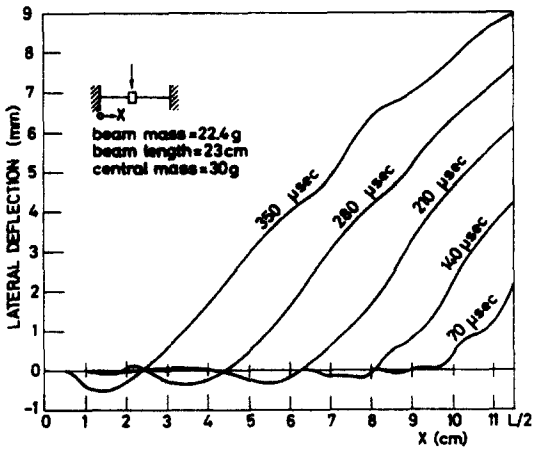

Fig. 10. Deflection of a fully clamped elastic-viscoplastic, strain hardening titanium beam with a central mass, at different times, subjected to a projectile impact and imbedment in the mass.

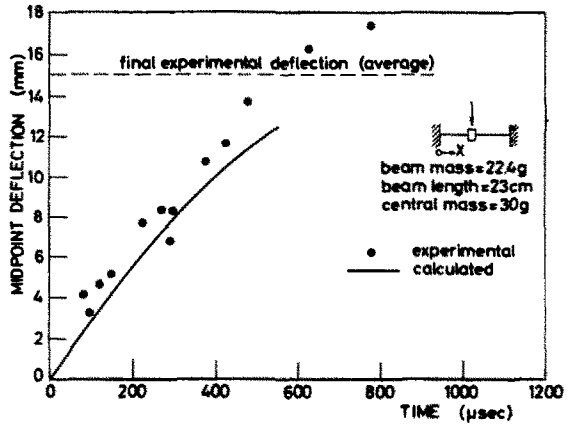

Fig. 11. Midpoint deflection of a fully clamped elastic-viscoplastic, strain hardening titanium beam with a central mass, subjected to a projectile impact and imbedment in the mass.

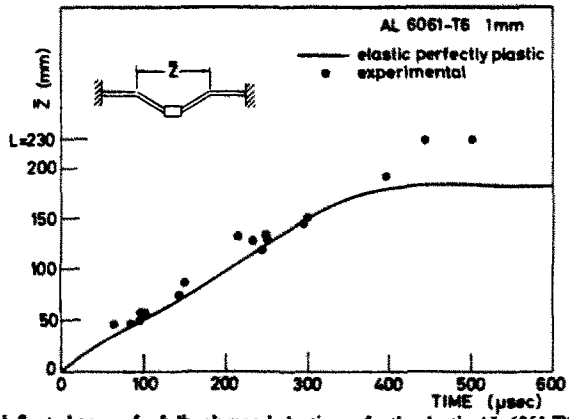

Fig. 12. Length of deflected zone of a fully clamped elastic-perfectly plastic AL 6061-T6 beam with a central mass, subjected to a projectile impact and imbedment in the mass.

Numerical stability

Numerical computational stability requires satisfaction of a relation between the time increment ΔT and the segment length δX. In solving simple elastic vibration problems directly using the differential equation of the elastic beam, the stability condition is found analytically [13],

$$a\Delta T/(\delta X)^2 < 1/2 \tag{27}$$

where

$$a = \sqrt{(EI/\rho A)}. \tag{28}$$

As "a" includes the elastic wave velocity, it is obvious that ΔT must decrease if the phenomenon goes faster. Usually, the number of segments is chosen according to the desired accuracy and only later is ΔT evaluated.

This criterion is, however, not suitable for the general program of large deflections. It also is not applicable in the present case even for elastic behavior, which takes place when the loads acting on the beam are sufficiently low, because the numerical scheme used in this investigation is different.

It was suggested [5] to use the experimental relation

$$(\Delta T/\delta X)\sqrt{(E/\rho)} < r$$

where r is a constant with a value between 0.5 and 0.8, but this relation does not take into

account the shape and dimensions of the cross section, the boundary conditions of the specific problem, and the constitutive equations of the material.

In the present paper, ΔT was found by trial and error by decreasing it until stability was achieved. The beam was divided into 40 equal segments. For examples A and B, the values obtained were respectively

$$\Delta T_A \simeq 0.2\ \mu\text{sec}$$
$$\Delta T_B \simeq 0.002\ \mu\text{sec}.$$

Both ΔT_A and ΔT_B are much less than the values corresponding to (27), and the computation is, therefore, relatively long and expensive. The computations were performed on an IBM 370/165. It was observed that the elastic-viscoplastic, strain hardening model had better stabilizing qualities than the elastic perfectly plastic one which may be considered an important advantage of this model.

Acknowledgements—The authors to thank Prof. S. R. Bodner for his valuable advice and suggestions during the research. The contributions of Dr. J. Awerbuch to the experimental work are gratefully acknowledged.

REFERENCES

1. E. W. Parkes, The permanent deformation of an Encastré beam struck transversely at any point in its span. *Proc. Inst. Civil Engineers* **10**, 277–304 (1958).
2. T. Nonaka, Some interaction effects in a problem of plastic beam dynamics. *J. Appl. Mech.* **34**, 623–640 (1967).
3. P. S. Symonds, Survey of methods of analysis for plastic deformation of structures under dynamic loading. *Tech. Rep.* Brown University to Dept. of the Navy, Office of Naval Research (1967).
4. J. W. Leech and T. H. H. Pian, Dynamic response of shells to externally-applied dynamic loads. *Report No.* ASD-TDR-62-610 Air Force Flight Dynamics Lab., Wright-Patterson AFB, Ohio (1962).
5. E. A. Witmer, H. A. Balmer, J. W. Leech and T. H. H. Pian, Large dynamic deformations of beams, rings, plates and shells. *AIAA J.* **1**, 1848–1857 (1963).
6. U. S. Lindholm, *Mechanical Properties at High Rates of Strain*, Chap. 1. Conference Series No 21, The Inst. of Physics, London and Bristol (1974).
7. J. D. Cambell, Dynamic plasticity: macroscopic and microscopic aspects. *Mater. Sci. Engng* **12**, 3–21 (1973).
8. S. R. Bodner and Y. Partom, Constitutive equations for elastic viscoplastic strain hardening materials. *J. Appl. Mech.* **42**, 379 (1975).
9. S. R. Bodner and Y. Partom, A large deformation elastic viscoplastic analysis of a thick walled spherical shell. *J. Appl. Mech.* **39**, 751–757 (1972).
10. S. R. Bodner and P. S. Symonds, Experimental and theoretical investigation of the plastic deformation of cantilever beams subjected to impulsive loading. *J. Appl. Mech.* **29**, 719–728 (1962).
11. T. Nicholas, Strain rate and strain-rate-history effects in several metals in torsion. *Experimental Mechanics* **11**, 370–374 (1971).
12. A. L. Florence and R. D. Firth, Rigid-plastic beams under uniformly distributed impulses. *J. Appl. Mech.* **32**, 481–488 (1965).
13. R. D. Richtmyer and K. W. Morton, *Difference Methods for Initial-Value Problems*, 2nd Edn. Interscience, New York (1967).